

Cite this: *Phys. Chem. Chem. Phys.*, 2011, **13**, 240–252

www.rsc.org/pccp

PAPER

A crossed molecular beam study on the reaction of methylidyne radicals [CH($X^2\Pi$)] with acetylene [$C_2H_2(X^1\Sigma_g^+)$]*—*competing $C_3H_2 + H$ and $C_3H + H_2$ channels

Pavlo Maksyutenko, Fangtong Zhang, Xibin Gu and Ralf I. Kaiser*

Received 18th August 2010, Accepted 18th October 2010

DOI: 10.1039/c0cp01529f

We carried out the crossed molecular beam reaction of ground state methylidyne radicals, CH($X^2\Pi$), with acetylene, $C_2H_2(X^1\Sigma_g^+)$, at a nominal collision energy of 16.8 kJ mol^{-1} . Under single collision conditions, we identified both the atomic and molecular hydrogen loss pathways forming C_3H_2 and C_3H isomers, respectively. A detailed analysis of the experimental data suggested the formation of *c*- C_3H_2 ($31.5 \pm 5.0\%$), $HCCCH/H_2CCC$ ($59.5 \pm 5.0\%$), and *l*- $HCCC$ ($9.0 \pm 2.0\%$). The reaction proceeded indirectly *via* complex formation and involved the unimolecular decomposition of long-lived propargyl radicals to form *l*- $HCCC$ plus molecular hydrogen and $HCCCH/H_2CCC$ plus atomic hydrogen. The formation of *c*- C_3H_2 was suggested to be produced *via* unimolecular decomposition of the cyclopropenyl radical, which in turn could be accessed *via* addition of the methylidyne radical to both carbon atoms of the acetylene molecule or after an initial addition to only one acetylenic carbon atom *via* ring closure. This investigation brings us closer to unraveling of the reaction of important combustion radicals—methylidyne—and the connected unimolecular decomposition of chemically activated propargyl radicals. This also links to the formation of C_3H and C_3H_2 in combustion flames and in the interstellar medium.

1. Introduction

The energetics and dynamics of reactions of resonantly stabilized free radicals (RSFRs) are of paramount importance in untangling the formation of soot particles,^{1–3} polycyclic aromatic hydrocarbons (PAHs) and their hydrogen deficient precursors from the ‘bottom up’ in combustion processes.^{3–15} In RSFRs, such as propargyl (C_3H_3 ; X^2B_1), allyl (C_3H_5 ; X^2A_2), 1-buten-3-yn-1-yl (C_4H_3 ; X^2A'), and the 2,4-pentadiynyl-1 radical (C_5H_3 ; X^2B_1) (Fig. 1), the unpaired electron is delocalized and spread out over two or more sites in the molecule. This results in a number of resonant electronic structures of comparable importance. Owing to the delocalization, resonantly stabilized free hydrocarbon radicals are more stable than ordinary radicals^{16–18} and can reach high concentrations in flames. These high concentrations make them important reactants to be involved in the formation of soot and PAHs. Combustion models suggest that the synthesis of small carbon-bearing molecules and radicals is linked to the formation of PAHs and to the production of soot in hydrocarbon flames.^{19–24} Reaction mechanisms currently in favor are thought to involve RSFRs like propargyl.^{9,12,25–39} The self-reaction of propargyl is considered to be one of the most significant cyclization steps in flames of aliphatic fuels.^{40–46} Electronic structure calculations imply that the acyclic

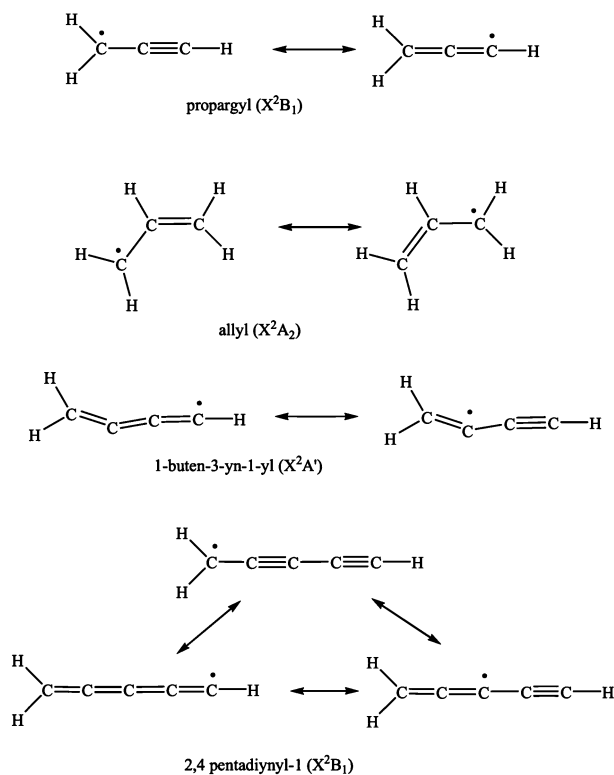


Fig. 1 Resonant structures of propargyl, allyl, 1-buten-3-yn-1-yl, and 2,4-pentadiynyl-1.

Department of Chemistry, University of Hawaii at Manoa, Honolulu, HI 96822, USA. E-mail: ralfk@hawaii.edu

collision complex(es) initially formed in the recombination of two propargyl radicals may isomerize ultimately forming benzene which decomposes to the phenyl radical plus a hydrogen atom.^{47,48} The models suggest further that consecutive reactions of the phenyl radical with unsaturated hydrocarbons can form more complex structures, possibly bicyclic aromatic hydrocarbon molecules like indene (C_9H_8) and naphthalene ($C_{10}H_8$).^{49–52}

Although the propargyl radical represents the most studied RSFR due to its potential role in the formation of the first aromatic ring in hydrocarbon flames, its stability and hence unimolecular decomposition has been poorly understood so far.^{42,44,48,53–65} Here, the unimolecular decomposition of propargyl⁶⁶ has been suggested to form predominantly C_3H_2 isomers cyclopropenylidene ($c-C_3H_2$; X^1A_1), propargylene (HCCCH; X^3B), and vinylidene carbene (H_2CCC ; X^1A_1)

(Fig. 2).^{33,43,67–77} These isomers present also important building blocks in the formation of PAHs and related molecules due to the equilibrium reaction with hydrogen atoms, which access the C_3H_3 surface *via* the generic process $C_3H_2 + H \leftrightarrow C_3H_3$.⁷⁸ In this context it is very important to highlight that Hansen *et al.* assigned propargylene (HCCCH) and cyclopropenylidene ($c-C_3H_2$) in cyclopentene flames *via* photoionization mass spectrometry.⁷⁹ A re-analysis of previous flame studies^{80–83} suggested that the nature of the C_3H_2 isomers formed critically depended on the hydrocarbon fuel.

Besides flame studies, the formation of C_3H_2 isomers was also studied experimentally and theoretically by investigating the unimolecular decomposition of chemically activated C_3H_3 molecules formed in the reaction of methylidyne radicals, $CH(X^2\Pi)$, with acetylene, C_2H_2 ($X^1\Sigma_g^+$), and of ground state carbon atoms, $C(^3P_1)$, with the vinyl radical, C_2H_3 (X^2A').

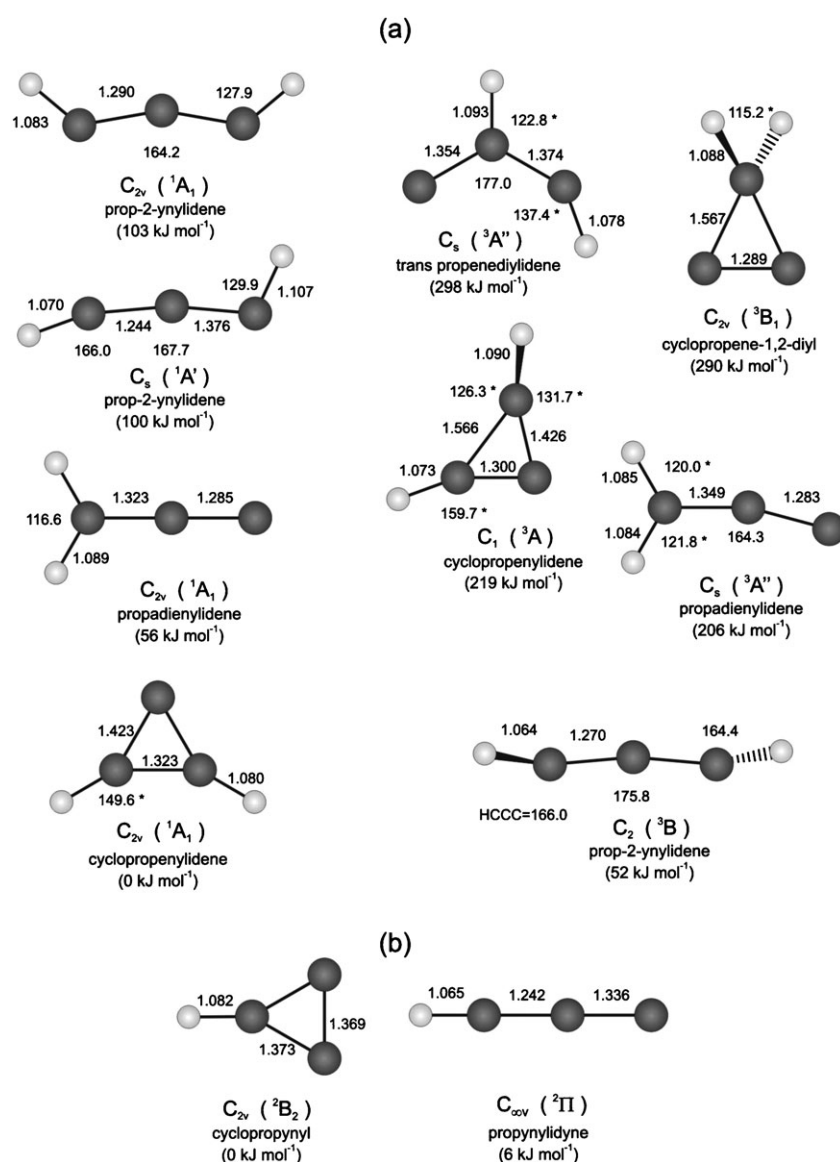


Fig. 2 Geometries of C_3H_2 (a) and C_3H (b) isomers; singlet and triplet spin states of the C_3H_2 isomers are grouped in the left and right column, respectively. The enthalpies of formation of the C_3H_2 and C_3H isomers are indicated relative to the lowest energy isomers (cyclopropenylidene and cyclopropynyl). Bond lengths are in angstroms and bond angles in degrees. Geometries and energies are compiled from Mebel *et al.*⁸⁹ Dimensions with asterisk (*) are taken from Peeters *et al.*⁸⁶

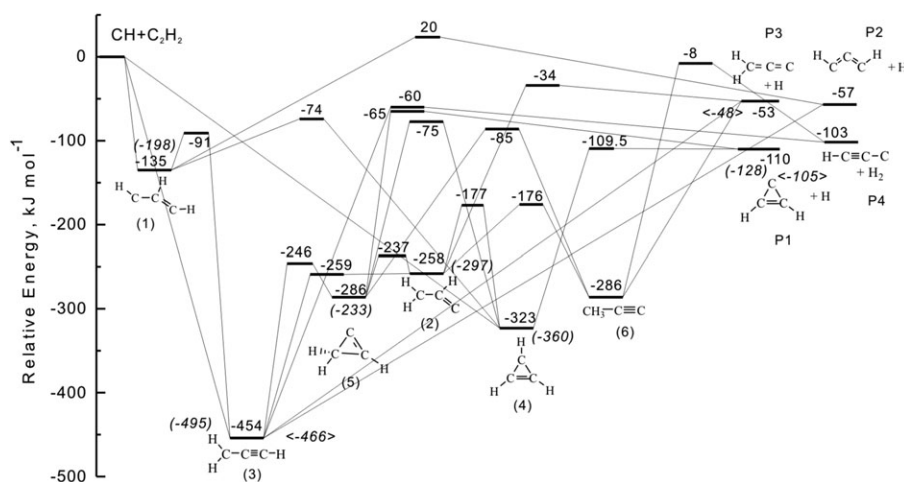


Fig. 3 Potential energy diagram of the reaction of methylidyne radicals with acetylene compiled from Mebel *et al.*,⁸⁹ Goulay *et al.*⁹⁰ (values in round brackets), and Vazquez *et al.*¹³² (values in angle brackets).

Most of the attention has been focused on the reaction of the methylidyne radical; this species presents one of the most reactive carbon-bearing radicals with unsaturated hydrocarbons holding rate constants of a few $10^{-10} \text{ cm}^3 \text{ s}^{-1}$.^{84,85} It possesses a Π symmetric vacant, non-bonding molecular orbital which is localized at the carbon atom directed perpendicular to the C–H bond. This empty orbital suggests that the methylidyne radical acts as a Lewis acid in reactions with unsaturated hydrocarbons such as acetylene. Nevertheless, no conclusion has been reached on the reaction mechanism of the methylidyne radical with acetylene to form distinct C_3H_3 isomers. Three entrance channels have been considered (Fig. 3): (i) an insertion into a carbon–hydrogen bond leading to the propargyl radical (3), (ii) addition to a single carbon atom forming 1-propene-1-yl-3-ylidene (1), and (iii) cycloaddition to the π -electron system leading to cycloprop-2-enyl (4). The initial collision complexes can undergo multiple isomerization and fragment *via* atomic and molecular hydrogen loss forming C_3H_2 and C_3H isomers, respectively. From the theoretical viewpoint, Peeters *et al.*⁸⁶ expanded a theoretical study by Walch *et al.* on the C_3H_3 PES⁸⁷ thus providing a detailed potential energy surface (PES) for the reaction at the B3LYP-DFT/6-31G** level of theory (Table 1). Accompanied by RRKM calculations,⁸⁸ the authors predicted that at pressures of up to several atmospheres, the initial insertion and cyclo addition had comparable probabilities, while the terminal addition pathway was insignificant ($<10\%$). Over a temperature range from 300 K to 2000 K, the triplet propargylene radical (HCCCH) was determined to be the dominant product (90–82%) followed by the thermodynamically more stable singlet cyclopropenylidene (*c*- C_3H_2) isomer (7–11%). The formation of singlet vinylidene carbene (H_2CCC) was predicted to be only a minor channel ($\sim 1\%$) similar to the molecular hydrogen loss forming the linear C_3H molecule (propenylidyne; $\sim 2\%$). The latter pathway was found to have an exit barrier; the calculations give low yields of this channel despite the greater exoergicity by about 46 kJ mol^{-1} to form propargylene (HCCCH) plus atomic hydrogen. Vereecken and Peeters suggested a tight transition state for the molecular hydrogen loss, which has a comparable energy to

HCCCH plus atomic hydrogen, in contrast to a very loose variational transition state for HCCCH plus atomic hydrogen pathway. An earlier study by Walch *et al.*⁸⁷ yielded a similar hydrogen atom yield of 100%, but predicted exclusively singlet propargylene (H_2CCC) production; however, multiple reaction pathways were not considered in this study. A third theoretical study by Mebel *et al.*⁸⁹ predicted a similar trend as Peeters *et al.*; branching ratio of HCCCH + H (84–87%), *c*- C_3H_2 + H (10–13%), and H_2CCC + H ($\sim 1\%$) were predicted with the molecular hydrogen elimination to linear tricarbon hydride isomer of minor importance ($\sim 2\%$). This theoretical study located a transition state from the cyclic C_3H_3 isomer to form *c*- C_3H_2 + H, which could not be found by Peeters *et al.*⁸⁶ The most recent high-level electronic structure and RRKM calculations predicted higher contributions of the *c*- C_3H_2 isomer (27.0%) *versus* triplet propargylene (HCCCH; 63.5%) with minor contributions from vinylidenecarbene (H_2CCC) plus atomic hydrogen and linear C_3H (HCCC) plus molecular hydrogen (less than 9.5% combined).⁹⁰

Experimentally, the unimolecular decomposition of C_3H_3 radicals can also be studied under molecular beam conditions *via* photodissociation of the propargyl radical. Photodissociation of the propargyl radical in the range of 242 to 248 nm generates the propargyl radical with a similar energy to that obtained *via* chemical activation in the reaction of methylidyne plus acetylene. Deyerl *et al.*⁹¹ used 242 nm to photodissociate internally cold propargyl radicals; the hydrogen atom products were ionized by Lyman- α radiation at 121 nm; Doppler profiles were analyzed to obtain the center-of-mass translational energy distribution. The peak close to zero translational energy suggests that electronic excitation is followed by internal conversion to the ground state surface followed by a statistical decay to the products. From the energetics, the authors concluded that the most likely product was cyclopropenylidene (*c*- C_3H_2). Photodissociation studies of isotopically substituted propargyl (D_2CCCH) radicals showed complete isotopic scrambling. The authors suggested a unimolecular decomposition of a $\text{C}_3\text{H}_2\text{D}$ intermediate formed *via* an internal^{1,2} hydrogen shift followed by cyclization. In a more recent study, Butler *et al.*⁹² examined the unimolecular

Table 1 Experimental and theoretical product branching ratios for the reaction of methylidyne radicals with acetylene and photodissociation studies of the propargyl radical^a

Reference	Method	Temperature, pressure	Branching ratio
Walch <i>et al.</i> (1998) ⁸⁷	RRKM on internally confined CI PES	1000 K, 0 Torr	100% CCCH ₂ + H
Vereecken and Peeters (1999) ⁸⁸	RRKM on B3LYP-DFT PES	1400 K*, 0 Torr	86% HCCCH + H 9% c-C ₃ H ₂ + H 3.3% HCCC + H ₂ 1.7% CCCH ₂ + H
Mebel <i>et al.</i> (2001) ⁸⁹	RRKM on B3LYP and RCCSD(T) PES	0 K, 0 Torr	84.5–87% HCCCH + H 10.2–12.8% c-C ₃ H ₂ + H 1.8–1.9% HCCC + H ₂ 0.9% CCCH ₂ + H
Goulay <i>et al.</i> (2009) ⁹⁰	RRKM on CBS-APNO PES	298 K, 0 Torr	27% c-C ₃ H ₂ + H 63.5% HCCCH + H <9.5% CCCH ₂ + H and C ₃ H + H ₂
Neumark <i>et al.</i> (2008) ⁹³	Photofragment translational spectroscopy of propargyl (248 nm)	0 K, 0 Torr	97.6 ± 1.2% H loss 2.4 ± 1.2% H ₂ loss
Mebel <i>et al.</i> (2001) ⁸⁹	Theoretical study of photodissociation of propargyl (193 nm)	0 K, 0 Torr	86.5% HCCCH + H 3.6% c-C ₃ H ₂ + H 5.5% HCCC + H ₂ 3.5% CCCH ₂ + H 0.9% C ₂ H ₂ + CH
	Theoretical study of photodissociation of propargyl (242 nm)	0 K, 0 Torr	90.2% HCCCH + H 5.1% c-C ₃ H ₂ + H 3% HCCC + H ₂ 1.6% CCCH ₂ + H 0.1% C ₂ H ₂ + CH
Boullart <i>et al.</i> (1996) ⁹⁶	Low pressure acetylene/atomic oxygen flame (600 K), threshold ionization MS	600 K, 2 Torr	85 ⁺¹⁵ ₋₉ H loss 15 ⁺⁹ ₋₁₅ H ₂ loss
McKee <i>et al.</i> (2003) ⁹⁷	Helium reaction flow, LIF of H atoms	295 K, 25 Torr	105 ± 9% H loss
Loison and Bergeat (2009) ⁸⁵	Helium reaction flow, LIF of H atoms	295 K, 2 Torr	90 ± 9% H loss
Goulay <i>et al.</i> (2009) ⁹⁰	Helium gas flow, tunable VUV (synchrotron) conformer-specific ionization of products; time-resolved MS	298 K, 4 Torr	>90% c-C ₃ H ₂ + H <10% HCCCH + H

^a branching ratios corresponding to our experimental collision energy are only shown

dissociation of propargyl (C₃H₃) over a wide range of internal energies. The authors proposed that H₂CCC is preferentially contributing on the fast side of the time-of-flight (TOF) distribution; c-C₃H₂ is likely the dominant isomer formed in the dissociation of propargyl radicals with energies near the dissociation threshold. A photodissociation study of propargyl at 248 nm by Neumark *et al.*⁹³ suggested that the propargyl radical fragments *via* atomic and molecular hydrogen loss with branching ratios of about 97.6 to 2.4. Under these conditions, theory predicts that only 5% of the atomic hydrogen loss produces cyclo propenylidene (c-C₃H₂) with propargylene (HCCCH) being dominant.⁹³ The $P(E_T)$ distribution of the molecular hydrogen loss leading to the C₃H product was distinct from the atomic hydrogen loss; it peaked away from zero translational energy at about 76 kJ mol⁻¹, with a high energy tail extending to about 112 kJ mol⁻¹ as characteristic for the formation of C₃H products. This distribution is indicative of a unimolecular decomposition of a C₃H₃ intermediate *via* a tight exit transition state. Unfortunately, the center-of-mass translational energy distribution ($P(E_T)$) of the C₃H₂ and C₃H products at $m/z = 38$ and 37 could not distinguish well between the isomers, except for the small amount of signal at $m/z = 38$ of 4 ± 2% with translational energy above the maximum for the propargylene (HCCCH) plus atomic hydrogen products; these were suggested to originate from the c-C₃H₂ isomer. A theoretical study of propargyl photodissociation at 193 and 242 nm by

Mebel *et al.*⁸⁹ supports the overall branching ratio of the atomic *versus* molecular hydrogen loss (97%/3%) measured by Neumark *et al.* at 242 nm and predicts a ~5% contribution of c-C₃H₂ and 1.6% of H₂CCC.

Alternatively, the reaction of methylidyne radicals with acetylene was also investigated in kinetics studies indicating a barrier-less addition of methylidyne to the acetylene molecule.^{84,94,95} Canosa *et al.*⁸⁴ investigated the temperature dependence of the global rate constant down to 23 K; their data supported the absence of any entrance barrier; however, this work could not determine any reaction product. Kinetic studies in gas flow tubes presented ambiguous results. For an elevated temperature of 600 K and 2 Torr, Boullart *et al.*⁹⁶ suggested atomic and molecular hydrogen pathways leading to C₃H₂ and C₃H isomers of about 85% and 15%, respectively, as derived from isothermal discharge flow reactor studies. However, McKee *et al.* employing the detection of hydrogen atoms *via* laser induced fluorescence (LIF) indicated an almost exclusive formation of C₃H₂ molecules of unknown structure.⁹⁷ On the other hand, Loison and Bergeat reported in a low-pressure fast flow reactor study that the hydrogen atom loss channel contributes to only 90%.⁸⁵ The most recent kinetic study by Goulay *et al.*⁹⁰ was conducted in a slow flow reactor at 4 Torr at 293 K coupled with tunable vacuum ultraviolet (VUV) photoionization and time resolved mass spectrometry to monitor the products. An analysis of the photoionization efficiency curve permitted an isomer-specific

detection of the reaction products and allowed an estimation of the reaction product branching ratios. The raw data suggested a predominant fraction of the cyclic C_3H_2 isomer (90%) and about 10% propargylene (HCCCH). Electronic structure calculations on the C_3H_3 and C_3H_2D surfaces revealed the presence of facile hydrogen-atom assisted isomerization processes of the nascent C_3H_2 products, in particular propargylene (HCCCH), to the cyclic C_3H_2 isomer; note that under these experimental conditions, single collision conditions do not exist.

Summarized, the previous theoretical and experimental (kinetics, photodissociation) studies suggest that no complete picture has emerged on the unimolecular decomposition of propargyl radicals. Consequently, a high-level experimental investigation on the unimolecular decomposition of the propargyl radical is warranted to shed light on this issue. These are experiments under *single collision conditions*, in which particles of one supersonic beam are made to ‘collide’ only with particles of a second beam. The crossed molecular beam technique represents the most versatile approach in the elucidation of the energetics, dynamics, and potential energy surfaces (PES) of elementary reactions under single collision conditions without successive reactions of the nascent reaction products.^{98–101} Here, we present crossed molecular beam data on the reaction of ground state methylidyne radicals with acetylene (CH/C_2H_2) at a collision energy of 16.8 kJ mol^{-1} . These data are compared then with previous experimental and theoretical studies of this system in an attempt to gain a more coherent picture of the reaction of methylidyne radicals with acetylene. Our results can be placed in the context of hydrocarbon combustion,^{102,103,104–107} interstellar chemistry^{108–114} and the chemistry of hydrocarbon rich atmospheres of planets (Uranus, Neptune)¹¹⁵ and moons (Titan, Triton)^{116,117} where methylidyne reactions with acetylene are important.

2. Experimental

The crossed beam reactions of methylidyne, $CH(X^2\Pi)$, with acetylene, $C_2H_2(X^1\Sigma_g^+)$, were conducted in a universal crossed molecular beams machine under single collision conditions.^{118–121} We generated a pulsed supersonic beam of ground state methylidyne radicals, $CH(X^2\Pi)$, via photolysis of helium-seeded bromoform ($CHBr_3$). Helium gas (99.9999%; Gaspro) at a pressure of 2.2 atm was bubbled through a stainless steel container, which acted as a reservoir for the bromoform held at a temperature of 283 K. This resulted in seeding fractions of 0.12% bromoform in helium. This mixture was introduced into a pulsed piezoelectric valve operated at a repetition rate of 60 Hz, pulse widths of $80 \mu\text{s}$, and a peak voltage of -400 to -450 V . The output of an excimer laser (KrF, 248 nm, 60 mJ per pulse) was focused with a 1 meter lens downstream of the nozzle to an area of about 4 mm by 0.7 mm. Based on calibration with noble gases, we estimated that a few 10^{12} radicals cm^{-3} can be formed in the interaction region of the scattering chamber. Metastable species formed from the tight focus conditions during the photolysis with the 248 nm laser beam are one potential source of background interference. These neutral electronically highly excited species can travel within the beam and pass the QMS filter; they get field ionized by the high voltage doorknob target held at -22.5 kV in the detector. In order to eliminate them, we introduced an electrostatic plate in the region between the pulsed valve nozzle and the skimmer operated at -2000 V . The pulsed beam of the methylidyne radicals pass through a skimmer; a four-slit chopper wheel selects a part of this beam with a well-defined velocity. In the interaction region, this section of the pulse intercepts the most intense section of a pulsed acetylene beam perpendicularly. The peak velocities (v_p) and speed ratios (S) of the segments of the interacting beams together with corresponding collision energies and

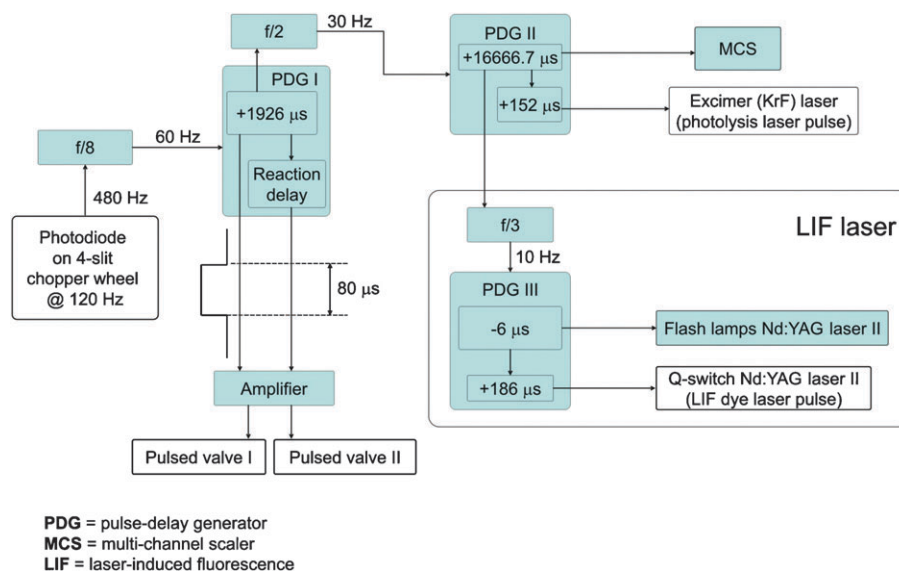


Fig. 4 Time sequence of the crossed beam experiments and LIF detection. The delay generator PDG I defines the time delay between the photodiode (time zero) and the pulsed valves; this delay generator triggers PDG II at a rate of 30 Hz. PDG II sets the delay for the excimer laser and—after division by three—triggers PDG III at 10 Hz; the latter triggers the Q-switch of the Nd:YAG laser utilized to pump the dye laser of the LIF laser system.

center-of-mass angles are $1747 \pm 17 \text{ ms}^{-1}$ and 17 ± 3 for methylidyne and $902 \pm 20 \text{ ms}^{-1}$ and 16 ± 1 for acetylene, respectively. This results in a nominal collision energy of $16.8 \pm 0.4 \text{ kJ mol}^{-1}$ and a center-of-mass angle of $45.9 \pm 0.9^\circ$. The time sequence of the experiment is shown in Fig. 4. Note that we determined the velocity and the speed ratio of the methylidyne radical beam on-axis in the TOF mode. Since signal at $m/z = 13$ (CH^+) also originates from dissociative ionization of non-photolyzed bromoform in the ionizer, even a *laser on minus laser off* subtraction cannot eliminate this contribution. Therefore, we utilized the electron impact ionizer in the *soft ionization* mode at an electron energy which still allowed sufficient signal from ionization of the methylidyne radical, but a significantly reduced signal from dissociative ionization of the bromoform precursor. The TOF spectra of the methylidyne beam were obtained at electron energy of 34 eV. Note that the photodissociation of bromoform is a multiphoton process initiated by the cleavage of the carbon–bromine bond to yield $\text{CHBr}_2 + \text{Br}^{122,123}$ ($\sigma(248 \text{ nm}) = 1.9 \times 10^{-18} \text{ cm}^2$).¹²⁴ Utilizing photoionization photofragment translational spectroscopy, North *et al.* observed also CHBr , CBr , HBr , and Br_2 fragments which were attributed to higher-order photodissociation processes of CHBr_2 and CHBr . Mebel computed the photodissociation cross sections of CHBr_2 and CHBr at 248 nm to form the methylidyne radical plus molecular and atomic bromine to be $1.6 \pm 0.4 \times 10^{-18}$ and $2.0 \pm 0.3 \times 10^{-18} \text{ cm}^2$, respectively.¹²⁵ Therefore, the photodissociation of bromoform produces apart from methylidyne radical possibly the reactive species CHBr_2 , CHBr , and CBr . When crossing with the acetylene beam, these systems have considerably lower center-of-mass angles due to the heavy bromine atom. For example, the CHBr fragment travelling with the same velocity as the methylidyne radical has a center-of-mass angle of only 8° compared to 45.9° in the methylidyne–acetylene system. Hence, the dynamics of bromine-containing radicals can be distinguished from those of the methylidyne reactions based on the distinct scattering angular ranges of the products and also by the different masses of the products.

The reactively scattered species were mass-filtered using a quadrupole mass spectrometric detector in the time-of-flight (TOF) mode after electron-impact ionization of the neutral molecules at 80 eV electron energy. The detector can be rotated within the plane defined by the primary and the secondary reactant beams to allow taking angular resolved TOF spectra. At each angle, up to 70 000 TOF spectra were accumulated to obtain good signal-to-noise ratios. The recorded TOF spectra were then integrated and normalized to extract the product angular distribution in the laboratory frame (LAB). In order to acquire information on the scattering dynamics, the laboratory data (TOF, LAB) were transformed into the center-of-mass reference frame utilizing a forward-convolution routine.^{126,127} This iterative method employs a parametrized or point-form angular flux distribution, $T(\theta)$, and translational energy flux distribution, $P(E_T)$, in the center-of-mass system (CM). Laboratory TOF spectra and the laboratory angular distributions (LAB) are calculated from the $T(\theta)$ and $P(E_T)$ functions and are averaged

over a grid of Newton diagrams accounting for the apparatus functions, beam divergences, and velocity spreads.

Only methylidyne radicals in the $^2\Pi$ ground electronic state participate in the reaction. The A and B states that might be populated in photolysis process have lifetimes of $440 \pm 20 \text{ ns}$ and $470 \pm 20 \text{ ns}$ ¹²⁸ and hence relax to the ground state before they reach the collision center. We characterized the rotational and vibrational modes of the methylidyne radical $\text{CH}(X^2\Pi)$ in the interaction region of the scattering chamber utilizing laser induced fluorescence (LIF). Methylidyne radicals are detected using $A^2\Delta-X^2\Pi$ transitions: (0,0) vibrational band for excitation near 431 nm and (0,1) band for detection near 490 nm. Laser light was produced by Lambda Physics Scanmate dye laser using Stilbene 420 dye pumped by the third harmonic (355 nm) of an integrated neodymium-doped yttrium aluminium garnet (Nd:YAG) laser. The output was attenuated to $\sim 10 \mu\text{J}$ to avoid saturation of the electronic transition. The interference filter (Andover corp., centered at 490 nm, 10 nm bandwidth) in front of the photomultiplier tube (PMT, Hamamatsu R955) discriminated against scattered laser light. The incoming detection laser beam is mainly absorbed by a piece of polished black glass (ThorLabs, neutral density filter, 40–20 surface quality), and the reflected part travels back into the baffles tube. The fluorescence spot in the interaction region is projected by a 35 mm focus lens onto the center of the iris in front of the PMT which is mounted on top and centered at the axis of QMS detector rotation. This vertical orientation of light detector minimizes the collection of Rayleigh scattered light of vertically polarized laser on the atoms and molecules in the beam. Another piece of polished black glass is placed under the interaction region onto the mount for the cold shield to minimize the propagation of scattered laser light in the light collection cone. The fluorescence signal detected by the PMT was then amplified by a built-in preamplifier of the Hamamatsu C7247 PMT socket assembly prior to feeding into a digital oscilloscope. Typically, 16 laser shots were averaged for each data point and sent to a computer *via* GPIB interface. An actual LIF spectrum of supersonic jet cooled methylidyne radicals is shown in Fig. 5. The spectrum was analyzed utilizing a LIFBASE database and spectral simulation for diatomic molecules by Jorge Luque.¹²⁹ Best fits were achieved with a rotational temperature of 14 K; the relative populations of the first vibrationally excited level ($\nu = 1$) was estimated to be less than 6% based on the (1,1), $R_1(1)$ peak. Note that we cannot distinguish between different spin–orbit states of methylidyne radical ($\Omega = 1/2$ vs. $\Omega = 3/2$) because for the observed transitions, the largest spectroscopic splitting (0.11 cm^{-1} for $R_2(1)$ transition) would be still smaller than the line width of the detection laser of 0.15 cm^{-1} .

3. Results

Scattering signal for the reaction of methylidyne with acetylene was monitored at mass-to-charge ratios (m/z) of 38 (C_3H_2^+), 37 (C_3H^+), and 36 (C_3^+); the time-of-flight (TOF) spectra and the corresponding laboratory angular distributions are shown in Fig. 6 and 7, respectively. Signal at $m/z = 38$ (C_3H_2^+) originates from the atomic hydrogen loss channel

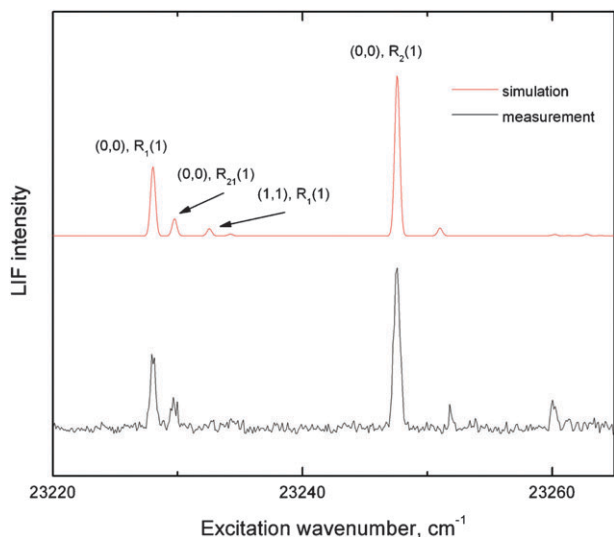


Fig. 5 LIF spectrum of methylidyne radicals in a supersonic helium beam (bottom) and the best-fit simulation (top). The simulation suggests a rotational temperature of 14 K; the relative populations of the first vibrationally excited level is less than 6%.

forming C_3H_2 isomers. The TOF and laboratory angular distribution for this channel could not be fit with a single channel, parametrized center-of-mass translational energy distribution ($P(E_T)$). However, a one channel fit could be achieved by successfully utilizing a $P(E_T)$ in point form and a parametrized center-of-mass angular distribution ($T(\theta)$). The TOF spectra at $m/z = 37$ (C_3H^+) are very interesting and after scaling—do *not* overlap with those obtained at $m/z = 38$. This finding alone suggests that signal at $m/z = 37$ does *not* only originate from dissociative electron impact ionization of the C_3H_2 parent molecules. In order to fit the laboratory data at $m/z = 37$ (C_3H^+), it was necessary to include two additional channels with the mass combination 37 amu (C_3H) plus 2 amu (H_2) from the methylidyne plus acetylene reactants and a second pathway with the mass combination 37 amu (C_3H) plus 1 amu (H). These findings deserve some comments. First, the need to incorporate the channel with the mass combination 37 amu plus 2 amu indicates that besides the methylidyne *versus atomic hydrogen* exchange pathway leading to molecules of the generic formula C_3H_2 , a second reaction channel to form C_3H isomer(s) *via molecular hydrogen* loss is also open. Secondly, it was imperative to include a reaction channel with the mass combination 37 amu plus 1 amu originating from reaction of ground state carbon atoms with acetylene to fit the data. Since the reaction dynamics of this system were studied in our group over a broad range of collision energies from 8 to 31 kJ mol^{-1} ,⁵⁷ the incorporation of this reaction channel does not present a complication. Note that due to the required tight laser focus necessary to generate methylidyne radicals in the primary source *via* multi photon dissociation of bromoform in the primary source chamber, this tight laser focus likely induced a photolysis of a fraction of the methylidyne radicals to generate ground state carbon atoms plus atomic hydrogen as well. Finally, let us have a look at the TOF data and laboratory angular distributions of $m/z = 36$ (C_3^+). It is obvious that neither the TOF nor the

LAB distribution of $m/z = 36$ overlaps with those obtained at $m/z = 37$ or 38. Therefore, we have to conclude that the signal at $m/z = 36$ does not originate solely from dissociative ionization of the C_3H_2 and C_3H parent molecules. A closer look at the TOF spectra depicts pronounced shoulders from about 200 to 250 μs ; these shoulders are also reflected in enhanced signal at the laboratory angular distribution of $m/z = 36$. This fast component could be fit with a product mass combination of 36 amu (C_3) plus 2 amu (H_2) originating from the reaction of ground state carbon atoms with acetylene. Recall the molecular hydrogen plus tricarbon channel was also observed previously in our group during the dynamics studies of the reaction of ground state carbon atoms plus acetylene. Therefore, the center-of-mass functions of this pathway were extracted from ref. 57 to adequately fit the laboratory data.

We would like to point out that although the laboratory data at $m/z = 38$ ($C_3H_2^+$) were nicely fit with a single channel utilizing center-of-mass translational energy and angular distributions in point and parameter form, respectively, we also investigated if a two-channel fit using all center-of-mass functions in parameter form could lead to an acceptable fit. This approach was guided by the results of the electronic structure calculations as compiled in Fig. 2 and the computed reaction energies to form the $c\text{-}C_3H_2$ isomer (exoergicity: 105–128 kJ mol^{-1}) and the $\text{HCCCH}/\text{H}_2\text{CCC}$ isomers (exoergicity: 48–57 kJ mol^{-1}). The results of the fits are overlaid in Fig. 6 and 7. The data at $m/z = 38$ could be nicely fit with a two-channel system accounting for the formation of $c\text{-}C_3H_2$ and $\text{HCCCH}/\text{H}_2\text{CCC}$; the corresponding center-of-mass functions are discussed below.

To summarize these findings, the laboratory data suggest that the reaction of methylidyne radicals with acetylene involves atomic and molecular hydrogen loss pathways leading to C_3H_2 and C_3H isomers as detected *via* $m/z = 38$ and 37. The scattering signal at $m/z = 38$ could be also fit with two channels representing the formation of two classes of isomers: $c\text{-}C_3H_2$ and $\text{HCCCH}/\text{H}_2\text{CCC}$. Following the procedure as outlined in ref. 57 we extracted the branching ratios of the products formed under single collision conditions in the reaction of methylidyne radicals plus acetylene to be as follows: $c\text{-}C_3H_2$: $31.5 \pm 5.0\%$, $\text{HCCCH}/\text{H}_2\text{CCC}$: $59.5 \pm 5.0\%$, and HCCC : $9.0 \pm 2.0\%$.

4. Discussion

To provide information on the reaction dynamics, we have to analyze the derived center-of-mass functions as compiled in Fig. 8. Please note that we discuss only those functions relevant to the reaction of methylidyne radicals with acetylene; the atomic carbon–acetylene system, whose center-of-mass functions were necessary to fit data at $m/z = 37$ and 36, was disseminated previously and the reader is referred to the original literature.⁵⁷ Let us investigate the center-of-mass translational energy distributions first. The $P(E_T)$ of the one-channel depicts a high energy cutoff at $118 \pm 8 \text{ kJ mol}^{-1}$. For those molecules born with no internal excitation, the maximum translational energy allowed presents the arithmetic sum of the collision energy and the absolute of the reaction exoergicity. Accordingly, the reaction exoergicity can be

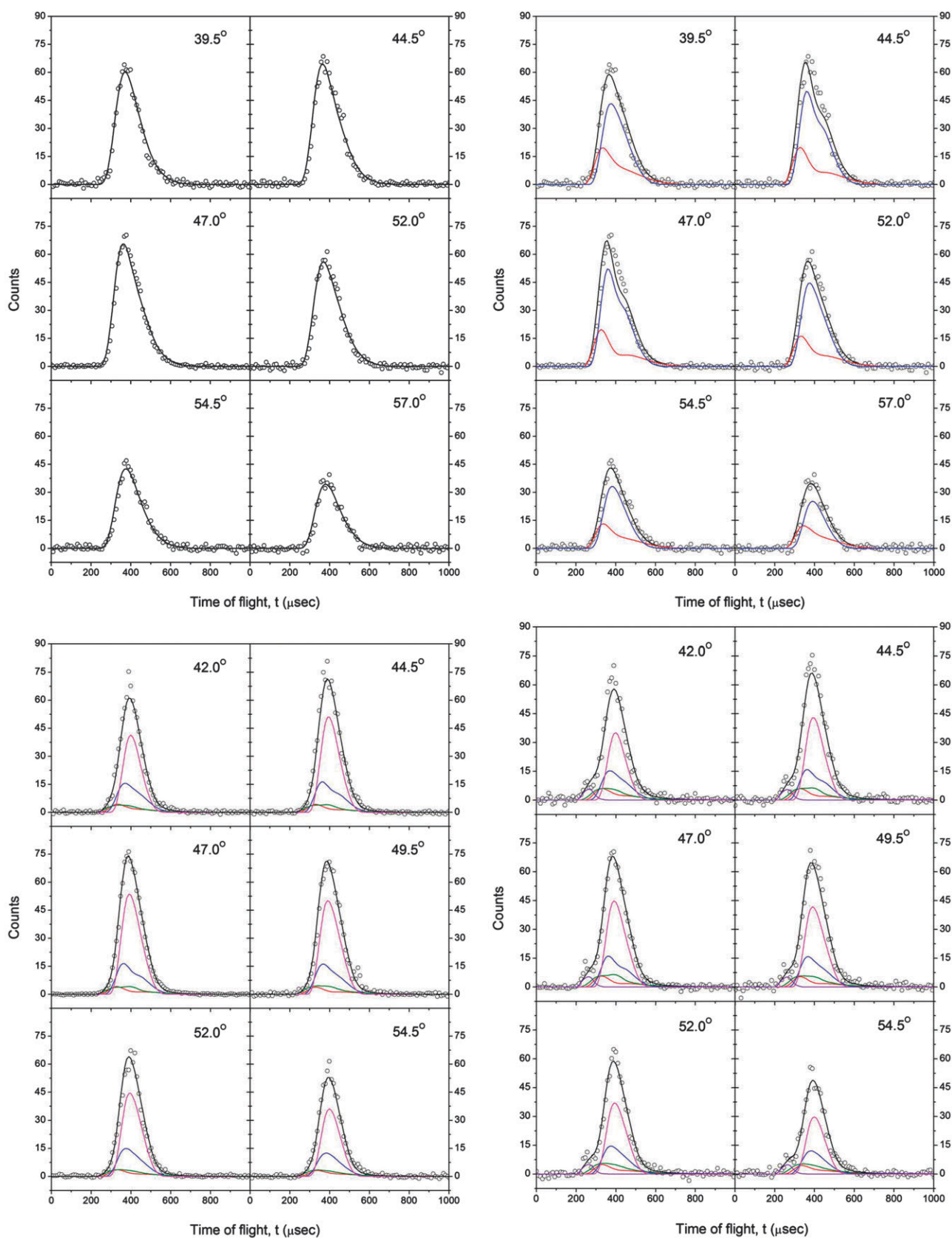


Fig. 6 TOF spectra recorded during the reaction of methylidyne radicals with acetylene. Top left $m/z = 38$ ($C_3H_2^+$) (single channel fit), top right: $m/z = 38$ ($C_3H_2^+$) (two channels fit; red: $c-C_3H_2$; blue: $HCCCH/H_2CCC$; black: sum), bottom left: $m/z = 37$ (C_3H^+ ; red: fragmentation from $c-C_3H_2$; blue: fragmentation from $HCCCH/H_2CCC$; olive: $C_3H + H_2$; magenta: $C_3H + H$; black: sum), bottom right: $m/z = 36$ (C_3^+ ; violet: $C_3 + H_2$). The open circles are the experimental data, the solid lines the fits.

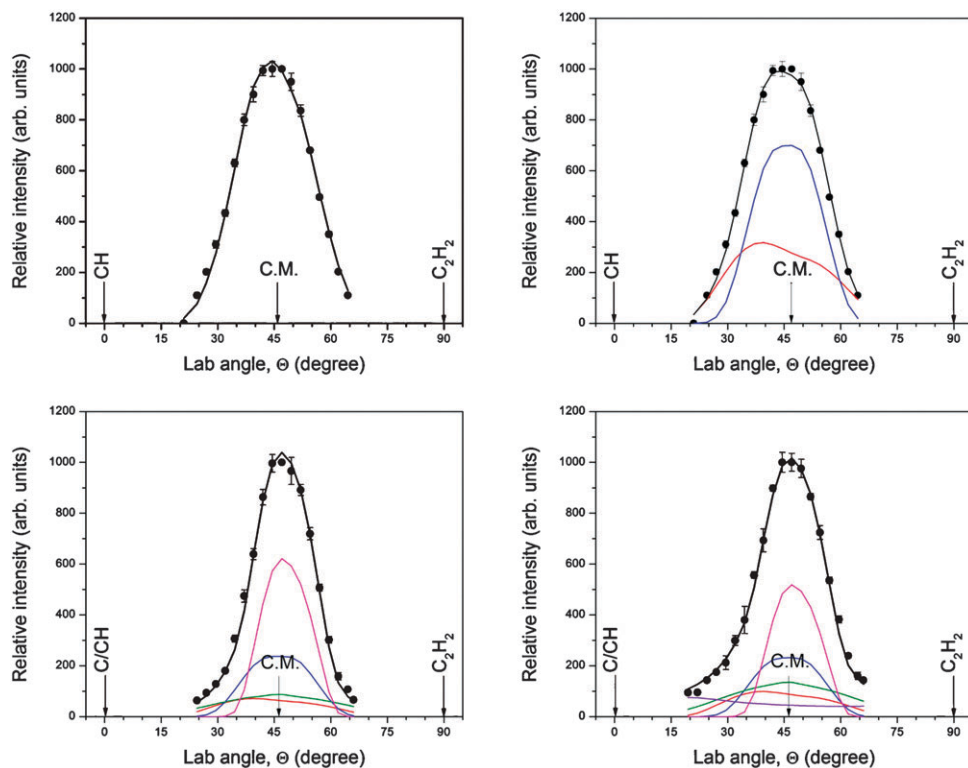


Fig. 7 Laboratory angular distributions of scattering signal recorded during the reaction of methylidyne radicals with acetylene. Top left $m/z = 38$ ($C_3H_2^+$) (single channel fit), top right: $m/z = 38$ ($C_3H_2^+$) (two channels fit), bottom left: $m/z = 37$ (C_3H^+), bottom right: $m/z = 36$ (C_3^+). C.M. indicates the center-of-mass angle of the reaction of methylidyne with acetylene. The circles are the experimental data, the solid lines the fits. The color code is identical to Fig. 6.

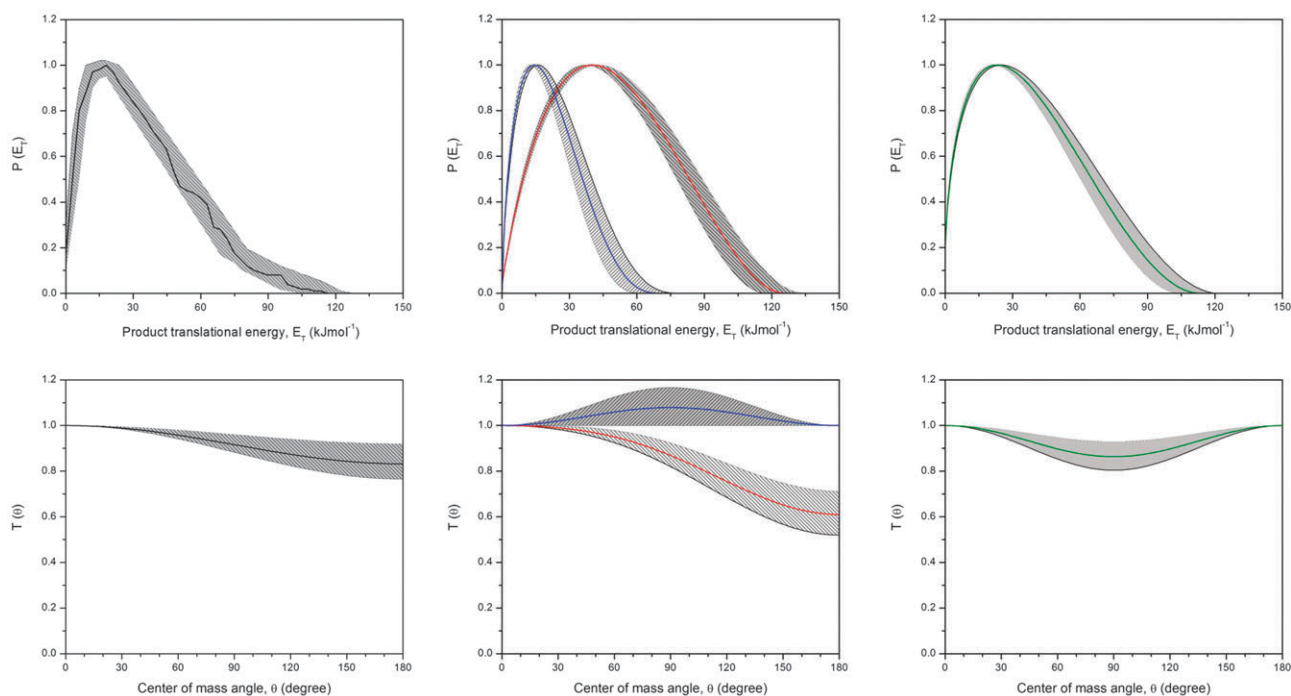


Fig. 8 Center-of-mass translational energy (top row) and angular distributions (bottom row) derived for the reaction channels in the methylidyne-acetylene system. Left column: one-channel fit of the C_3H_2 (38 amu) plus atomic hydrogen (1 amu) channel; center column: two channel fits of the C_3H_2 (38 amu) plus atomic hydrogen (1 amu) channel, blue: $HCCCH/H_2CCC$ isomer, red: $c-C_3H_2$ isomer, right column: molecular hydrogen elimination channel leading to C_3H isomer(s) (37 amu). The hatched areas define the acceptable fits within the experimental error limits.

determined by subtracting the collision energy from the maximum translational energy observed to be $101 \pm 8 \text{ kJ mol}^{-1}$. A comparison of this value with those computed for distinct C_3H_2 isomers suggests the formation of at least the thermodynamically most stable $\text{c-C}_3\text{H}_2$ molecule. Further, the $P(E_T)$ peaks away from zero translational energy; no acceptable fits were achieved with monotonically decreasing functions peaking at zero translational energy. This pattern suggests the existence of a tight exit transition state upon formation of $\text{c-C}_3\text{H}_2$ plus atomic hydrogen or alternatively dynamical effects as the consequence of the gas phase bimolecular collision. Recall that we were able to split up the one-channel fit into two channels (Fig. 8, center column). As evident from the fits of the laboratory data, both the one and the two channel fits nicely replicate the experimental data. The corresponding two channel fit was achieved with $P(E_T)$ s extending to maxima of $73 \pm 7 \text{ kJ mol}^{-1}$ and $120 \pm 10 \text{ kJ mol}^{-1}$. A subtraction of the collision energy leads to reaction exoergicities of $56 \pm 7 \text{ kJ mol}^{-1}$ and $103 \pm 10 \text{ kJ mol}^{-1}$, respectively. These values are in good agreement with those attributable to the formation of the $\text{HCCCH}/\text{H}_2\text{CCC}$ (channel 1) and the $\text{c-C}_3\text{H}_2$ isomers (channel 2) by comparison with the computed exoergicities of 48–57 kJ mol^{-1} and 105–128 kJ mol^{-1} , respectively. Note that within the error limits, we cannot discriminate between the HCCCH and H_2CCC isomers, with the latter energetically slightly unfavorable. It is also important to indicate that the $P(E_T)$ related to the formation of the $\text{HCCCH}/\text{H}_2\text{CCC}$ isomer(s) peaks closer to zero at 10–20 kJ mol^{-1} than the function accounting for the $\text{c-C}_3\text{H}_2$ molecule which shows a distribution maximum at about 35–50 kJ mol^{-1} . Therefore, either the transition state leading to $\text{c-C}_3\text{H}_2$ is tighter compared to those leading to $\text{HCCCH}/\text{H}_2\text{CCC}$ or dynamical effects are more pronounced in the formation of the $\text{c-C}_3\text{H}_2$ isomer. Having accounted for the atomic hydrogen channel, we are turning our attention now to the molecular hydrogen loss pathway. Here, the $P(E_T)$ extends to translational energies of $115 \pm 8 \text{ kJ mol}^{-1}$; a subtraction of the collision energy results in an exoergicity of $98 \pm 8 \text{ kJ mol}^{-1}$, to form the linear C_3H isomer, which is in close agreement with the theoretically predicted value of 103 kJ mol^{-1} (Fig. 3). Likewise, this distribution peaks well away from zero translational energy at about 25–30 kJ mol^{-1} indicating a tight exit transition state involved in the formation of $\text{l-C}_3\text{H}$ plus molecular hydrogen. Note that the calculations suggest that the cyclic C_3H isomer cannot be formed in the reaction of methylidene with acetylene. The translational energy distributions also allow for the determination of the percentage of available energy partitioned into the translational degrees of freedom. These values were determined to be $39 \pm 5\%$ for $\text{c-C}_3\text{H}_2$, $30 \pm 3\%$ for $\text{HCCCH}/\text{H}_2\text{CCC}$, and $35 \pm 3\%$ for the linear C_3H isomer—fractions which indicate indirect scattering dynamics involving collision complexes.¹³⁰

The center-of-mass angular distributions reveal important additional information on the reaction dynamics. Upon first inspection, we notice that for all channels, intensity of the center-mass angular distributions is always greater than zero for all angles. This finding implies rather indirect scattering dynamics involving C_3H_3 intermediates. Secondly, the angular

distributions leading to $\text{HCCCH}/\text{H}_2\text{CCC}$ and $\text{l-C}_3\text{H}$ are forward–backward symmetric about 90° . The symmetry suggests that the intermediate has a lifetime longer than the rotational period of the decomposing complex.¹³⁰ Most importantly, data for the molecular elimination channel leading to $\text{l-C}_3\text{H}$ could be only fit with a $T(\theta)$ with a minimum at 90° . This indicates geometrical constraint upon complex decomposition with the molecular hydrogen being emitted preferentially within the rotation plane of the decomposing C_3H_3 intermediate almost perpendicularly to the total angular momentum vector.¹³⁰ The channel leading to $\text{HCCCH}/\text{H}_2\text{CCC}$ involved isotropic or slightly peaking center-of-mass angular distributions. However, the $T(\theta)$ leading to $\text{c-C}_3\text{H}_2$ plus atomic hydrogen is distinct from the previously discussed functions as it shows a slight forward peaking. Ratios of the flux intensities at the respective maxima and minima, $I(0^\circ)/I(180^\circ)$, were found to be 1.3 ± 0.2 indicating the possible existence of an osculating complex which decomposes to $\text{c-C}_3\text{H}_2$ plus atomic hydrogen. Further, the incorporated methylidyne radical and the leaving hydrogen atom have to be located on opposite sides of the rotational axis to account for this forward scattering.

Having analyzed the derived center-of-mass functions, we are proposing now the underlying chemical dynamics leading to the formation of $\text{c-C}_3\text{H}_2$, $\text{HCCCH}/\text{H}_2\text{CCC}$, and $\text{l-C}_3\text{H}$ by combining our results with those obtained from recent electronic structure calculations as compiled in Fig. 3. For this, we are correlating the structures of the reaction products with the intermediates involved and also with the experimentally found dynamics. The results suggest that the propargyl radical intermediate (3) presents the central decomposing intermediate forming $\text{HCCCH}/\text{H}_2\text{CCC}$ plus atomic and $\text{l-C}_3\text{H}$ plus molecular hydrogen *via* a complex-forming reaction mechanism (indirect scattering dynamics as predicted by the center-of-mass angular distributions). Here, propargyl can undergo unimolecular decomposition *via* molecular hydrogen loss leading to the $\text{l-C}_3\text{H}$ isomer plus molecular hydrogen through a tight exit transition state located about 43 kJ mol^{-1} above the energy of the separated reactants. The computed geometry of the exit transition state⁸⁶ suggests that molecular hydrogen is ejected almost in the plane of the decomposing intermediate. Here, one hydrogen atom of the leaving molecular hydrogen was calculated to depart at an angle of about 1.1° below and the second hydrogen atom 7.4° above the molecular plane. This theoretical prediction is fully supported by our experimental finding of a $T(\theta)$ holding a minimum at 90° , *i.e.* a preferential emission of molecular hydrogen within the plane of the decomposing complex. Note that based on the PES, an alternative pathway connects intermediate CH_3CC (6) to $\text{l-C}_3\text{H}$ plus molecular hydrogen. This mechanism would also involve a tight exit transition state, which is located 95 kJ mol^{-1} above the separated reactants. However, the computed geometry of the transition state connecting intermediate (6) and $\text{l-C}_3\text{H}$ indicates that molecular hydrogen is lost perpendicularly to the rotational plane at an angle of about 86.7° . This clearly contradicts our experimental finding, and we can dismiss that intermediate (6) plays a role in the chemical dynamics of this channel. Therefore, we can conclude that the $\text{l-C}_3\text{H}$ plus molecular hydrogen are formed

via unimolecular decomposition of the propargyl radical, but not from intermediate (6). Recall further that the $T(\theta)$ of this channel is indicative of a long-lived complex; this can be rationalized by the deep potential energy well of 454 to 495 kJ mol^{-1} , in which the propargyl radical intermediate resides. To summarize, the existence of the propargyl radical (3), decomposing to $\text{l-C}_3\text{H}$ plus molecular hydrogen, can account for the experimental findings of a forward-backward symmetric center-of-mass angular distribution, an experimentally predicted tight exit transition state (recall that the $P(E_T)$ of this channel was found to peak away from zero translational energy in the range of 25–30 kJ mol^{-1}), and the in-plane emission of molecular hydrogen.

A closer look at the pertinent PES indicates that the propargyl radical (6) can—besides molecular hydrogen emission to form $\text{l-C}_3\text{H}$ —also fragment via atomic hydrogen elimination to H_2CCC and/or HCCCH via loose transition states. Since the transition state connecting (6) with $\text{l-C}_3\text{H}$ plus molecular hydrogen is almost isoenergetic with the energies of H_2CCC and/or HCCCH , but of tight nature compared to the loose transition states from propargyl via atomic hydrogen loss, we expect that the atomic hydrogen loss to H_2CCC and/or HCCCH dominates over the molecular hydrogen loss channel. This is confirmed by our experimental findings suggesting fractions of $59.5 \pm 5.0\%$ for $\text{HCCCH}/\text{H}_2\text{CCC}$, but only $9.0 \pm 2.0\%$ for l-HCCC . Further, the inherent center-of-mass angular distribution for the hydrogen atom loss channel leading to $\text{HCCCH}/\text{H}_2\text{CCC}$ suggested the existence of a long-lived reaction intermediate. Consequently, we can conclude that a long-lived propargyl radical presents a common reaction intermediate; its unimolecular decay leads predominantly to $\text{HCCCH}/\text{H}_2\text{CCC}$ via atomic and to a lesser amount to l-HCCC via molecular hydrogen loss pathways. However, we should point out that the $P(E_T)$ of the atomic hydrogen loss channel was found to peak at 10–20 kJ mol^{-1} . A long-lived complex behavior should be reflected in a $P(E_T)$ peaking at zero translational energy. Could other reaction intermediates also contribute to the atomic hydrogen loss and inherent formation of $\text{HCCCH}/\text{H}_2\text{CCC}$? Based on the PES, intermediate (1) could in principle decay to HCCCH plus atomic hydrogen. However, the inherent barrier of 155 kJ mol^{-1} cannot be verified experimentally. Likewise, if (1) is formed, it rather isomerizes to the propargyl intermediate (3) via a barrier of only 44 kJ mol^{-1} . Hence, we can exclude intermediate (1) as a source of HCCCH plus atomic hydrogen. On the other hand, intermediate (2), which could be formed via isomerization of (3) and/or (3) \rightarrow (5) \rightarrow (2) can connect to H_2CCC plus atomic hydrogen via a barrier located 9 to 14 kJ mol^{-1} above the energy of the separated products. Therefore, at the present stage, we cannot disregard that the decomposition of intermediate (2), which is formed from the already identified propargyl radical intermediate (3) via isomerization leads to H_2CCC plus atomic hydrogen.

Finally, we are addressing the possible dynamics to form the $\text{c-C}_3\text{H}_2$ molecule. The PES offers two possible routes. The first pathway proceeds via addition of the methylidyne radical to the carbon-carbon triple bond of the acetylene molecule forming a cyclic intermediate (4) which decomposes through a loose exit transition state. The second mechanism would

involve a decomposing intermediate (5), which is formed via isomerization of the propargyl radical. Recall that the propargyl radical was found to be long-lived with respect to its rotational period. On the other hand, the $T(\theta)$ is slightly forward-scattered and indicative of an osculating complex. Therefore, if $\text{c-C}_3\text{H}_2$ is formed from (5), and the latter from (3), we expect a forward-backward symmetric center-of-mass angular distribution. Therefore, we can conclude that intermediate (4) decomposed preferentially to $\text{c-C}_3\text{H}_2$. However, does the experimentally found off-zero-peaking of the corresponding $P(E_T)$ contradict the loose transition state predicted from calculations? It should be recalled that dynamical factor can lead to center-of-mass translational energy distributions peaking well away from zero translational energy. This was observed previously in the forward scattered channels involved in the formation of $\text{c-C}_3\text{H}$ and the propargyl isomer (C_3H_3) plus a light hydrogen atom co-fragment as observed in the crossed beam reaction of ground state carbon atoms with acetylene⁵⁷ and ethylene¹³¹ studied earlier. The off-zero peaking micro channels were also correlated with slightly forward-peaking center-of-mass angular distributions. Therefore, a comparison of the presently observed dynamics with those extracted for the $\text{c-C}_3\text{H} + \text{H}$ and $\text{C}_3\text{H}_3 + \text{H}$ channels in the $\text{C}(^3\text{P})/\text{C}_2\text{H}_2$ and $\text{C}(^3\text{P})/\text{C}_2\text{H}_4$ reactions indicates that in the $\text{CH}/\text{C}_2\text{H}_2$ system, the $\text{c-C}_3\text{H}_2$ is likely formed via a cyclic intermediate (4), which in turn is accessed via addition of the methylidyne radical to the carbon-carbon triple bond of the acetylene reactant. An analysis of the possible rotational axes of (4) suggests that a rotation around A/B axes can account for the forward scattering since in this case, the incorporated methylidyne reactant and the leaving hydrogen atom are located on opposite sides of the rotational axis.

How do our results of $\text{c-C}_3\text{H}_2$ ($31.5 \pm 5.0\%$), $\text{HCCCH}/\text{H}_2\text{CCC}$ ($59.5 \pm 5.0\%$), and HCCC ($9.0 \pm 2.0\%$) compare with previous experiments and calculations as compiled in Table 1? It is important to note that none of the prior experiments was conducted under single collision conditions. Nevertheless, the preceding experiments by Boullart *et al.*, McKee *et al.*, Loison *et al.*, and Goulay *et al.* agree with our finding that the atomic hydrogen loss channel ($105 \pm 9\%$ – $85 \pm 15\%$) dominates over the molecular hydrogen loss. Previous works suggested upper limits of about 10% by predominantly monitoring the hydrogen atom yield quantitatively with respect to a well-known reference system. Our crossed beam experiments, on the other hand, were able to explicitly verify the molecular hydrogen loss pathway directly by monitoring TOF spectra at $m/z = 37$ and by a comparison of their patterns and fits with those of $m/z = 38$ and 36. Based on the two channel fit, we were also able to estimate the branching ratios of the cyclic versus non-cyclic C_3H_2 isomers to be about 2 : 3. It should be recalled that based on our experimental data, we cannot discriminate between the HCCCH and H_2CCC isomers.

5. Summary and conclusion

We conducted the crossed molecular beam reaction of ground state methylidyne radicals, $\text{CH}(X^2\Pi)$, with acetylene, $\text{C}_2\text{H}_2(X^1\Sigma_g^+)$, at a collision energy of 16.8 kJ mol^{-1} . Under

single collision conditions, we identified both the atomic and molecular hydrogen loss pathways leading to C_3H_2 and C_3H isomers, respectively. A detailed analysis of the experimental data suggested the formation of $c-C_3H_2$ ($31.5 \pm 5.0\%$), $HCCCH/H_2CCC$ ($59.5 \pm 5.0\%$), and $l-HCCC$ ($9.0 \pm 2.0\%$) and identified for the first time the formation of C_3H_2 and C_3H isomers under single collision conditions. The reaction proceeds indirectly *via* complex formation and proceeds *via* unimolecular decomposition of long-lived propargyl radicals (**3**) to form $l-HCCC$ plus molecular hydrogen and $HCCCH/H_2CCC$ plus atomic hydrogen. The involvement of two higher energy, C_3H_3 intermediates (**5**) and (**2**) formed *via* isomerization of propargyl (**3**) cannot be discounted at the present stage. On the other hand, the $c-C_3H_2$ was suggested to be produced *via* unimolecular decomposition of the cyclopropenyl radical (**4**), which in turn can be accessed *via* addition of the methylidyne radical to both carbon atoms of the acetylene molecule or after an initial addition to only one acetylenic carbon atom *via* ring closure. Future studies will investigate the CH/C_2D_2 and CD/C_2H_2 systems to answer the remaining questions, such as the determination of an explicit branching ratio of $HCCCH$ versus H_2CCC and the role of higher energy C_3H_3 isomers (**5**) and (**2**). Nevertheless, our present studies bring us closer to the understanding of the reaction of important combustion radicals—methylidyne—and the connected unimolecular decomposition of chemically activated propargyl radicals. This also links to the formation of C_3H and C_3H_2 in combustion flames and in the interstellar medium.

Acknowledgements

This project was supported by the US Department of Energy Office of Science (DE-FG02-03-ER15411).

References

- C. C. Austin, D. Wang, D. J. Ecobichon and G. Dussault, *J. Toxicol. Environ. Health, Part A*, 2001, **63**, 437.
- A. Ergut, Y. A. Levendis, H. Richter, J. Carlson, Fourth Jt. Meet. U.S. Sect. Combust. Inst.: West. States, Cent. States, East. States, Philadelphia, PA, United States, Mar. 20–23, 2005, A05/1.
- A. Kazakov and M. Frenklach, *Combust. Flame*, 1998, **112**, 270.
- R. I. Kaiser, T. N. Le, T. L. Nguyen, A. M. Mebel, N. Balucani, Y. T. Lee, F. Stahl, P. v. R. Schleyer and H. F. Schaefer III, *Faraday Discuss.*, 2002, **119**, 51.
- J. Appel, H. Bockhorn and M. Frenklach, *Combust. Flame*, 2000, **121**, 122.
- C. E. Baukal, *Oxygen Enhanced Combustion*, 1998.
- M. F. Budyka, T. S. Zyubina, A. G. Ryabenko, V. E. Muradyan, S. E. Esipov and N. I. Cherepanova, *Chem. Phys. Lett.*, 2002, **354**, 93.
- F. Cataldo, Editor Polyynes: Synthesis, Properties, and Applications, Interdisciplinary Meeting on Polyynes and Carbyne held 30–31 October 2003 in Naples, Italy, 2006.
- M. Frenklach, *Phys. Chem. Chem. Phys.*, 2002, **4**, 2028.
- A. Kazakov and M. Frenklach, *Combust. Flame*, 1998, **114**, 484.
- Y.-T. Lin, R. K. Mishra and S.-L. Lee, *J. Phys. Chem. B*, 1999, **103**, 3151.
- A. Necula and L. T. Scott, *J. Am. Chem. Soc.*, 2000, **122**, 1548.
- A. M. Nienow and J. T. Roberts, *Annu. Rev. Phys. Chem.*, 2006, **57**, 105.
- H. Richter and J. B. Howard, *Prog. Energy Combust. Sci.*, 2000, **26**, 565.
- L. Vereecken, H. F. Bettinger and J. Peeters, *Phys. Chem. Chem. Phys.*, 2002, **4**, 2019.
- D. B. Atkinson and J. W. Hudgens, *J. Phys. Chem. A*, 1999, **103**, 4242.
- D. K. Hahn, S. J. Klippenstein and J. A. Miller, *Faraday Discuss.*, 2001, **119**, 79.
- D. J. Mann and W. L. Hase, *J. Am. Chem. Soc.*, 2002, **124**, 3208.
- A. B. Fialkov, J. Dennebaum and K. H. Homann, *Combust. Flame*, 2001, **125**, 763.
- K. J. Higgins, H. Jung, D. B. Kittelson, J. T. Roberts and M. R. Zachariah, *J. Phys. Chem. A*, 2002, **106**, 96.
- V. V. Kislov, A. M. Mebel and S. H. Lin, *J. Phys. Chem. A*, 2002, **106**, 6171.
- A. Kitajima, T. Hatanaka, M. Takeuchi, H. Torikai and T. Miyadera, *Combust. Flame*, 2005, **142**, 72.
- J. Kou, T. Mori, Y. Kubozono and K. Mitsuke, *Phys. Chem. Chem. Phys.*, 2005, **7**, 119.
- P. Mitchell and M. Frenklach, *Phys. Rev. E: Stat., Nonlinear, Soft Matter Phys.*, 2003, **67**, 061407.
- B. Apicella, R. Barbella, A. Ciajolo and A. Tregrossi, *Combust. Sci. Technol.*, 2002, **174**, 309.
- V. I. Babushok and A. W. Miziolek, *Combust. Flame*, 2004, **136**, 141.
- F. Battin-Leclerc, *Phys. Chem. Chem. Phys.*, 2002, **4**, 2072.
- G. A. Dolgonos and G. H. Peslherbe, *Int. J. Mass Spectrom.*, 2005, **241**, 261.
- N. S. Goroff, *Acc. Chem. Res.*, 1996, **29**, 77.
- K.-H. Homann, *Angew. Chem., Int. Ed.*, 1998, **37**, 2435.
- M. M. Maricq, *Combust. Flame*, 2004, **137**, 340.
- B. Oektem, M. P. Tolocka, B. Zhao, H. Wang and M. V. Johnston, *Combust. Flame*, 2005, **142**, 364.
- H. Richter and J. B. Howard, *Phys. Chem. Chem. Phys.*, 2002, **4**, 2038.
- L. Shebaro, S. R. Bhalotra and D. Herschbach, *J. Phys. Chem. A*, 1997, **101**, 6775.
- K. Siegmann and K. Sattler, *J. Chem. Phys.*, 2000, **112**, 698.
- R. Taylor, G. J. Langley, H. W. Kroto and D. R. M. Walton, *Nature*, 1993, **366**, 728.
- B. V. Unterreiner, M. Sierka and R. Ahlrichs, *Phys. Chem. Chem. Phys.*, 2004, **6**, 4377.
- C. L. Morter, S. K. Farhat, J. D. Adamson, G. P. Glass and R. F. Curl, *J. Phys. Chem.*, 1994, **98**, 7029.
- R. D. Kern, H. Chen, J. H. Kiefer and P. S. Mudipalli, *Combust. Flame*, 1995, **100**, 177.
- Y. Georgievskii, J. A. Miller and S. J. Klippenstein, *Phys. Chem. Chem. Phys.*, 2007, **9**, 4259.
- L. B. Harding, S. J. Klippenstein and J. A. Miller, *J. Phys. Chem. A*, 2008, **112**, 522.
- R. D. Kern and K. Xie, *Prog. Energy Combust. Sci.*, 1991, **17**, 191.
- J. A. Miller and C. F. Melius, *Combust. Flame*, 1992, **91**, 21.
- J. A. Miller, M. J. Pilling and J. Troe, *Proc. Combust. Inst.*, 2005, **30**, 43.
- J. A. Miller, J. P. Senosiain, S. J. Klippenstein and Y. Georgievskii, *J. Phys. Chem. A*, 2008, **112**, 9429.
- J. P. Senosiain, S. J. Klippenstein and J. A. Miller, *Proc. Combust. Inst.*, 2007, **31**, 185.
- C. F. Melius, J. A. Miller and E. M. Evleth, *Symp. (Int.) Combust.*, [Proc.], 1992, **24**, 621.
- J. A. Miller and S. J. Klippenstein, *J. Phys. Chem. A*, 2003, **107**, 7783.
- Here, PAHs may also form without involving six-membered aromatic precursors *via* reactions of polyacetylenes with C_4H_x species ($x = 1-5$) and through reactions of two C_5H_5 radicals followed by rearrangements and hydrogen emission(s) to form naphthalene and/or the azulene isomer.
- C. A. Arrington, C. Ramos, A. D. Robinson and T. S. Zwier, *J. Phys. Chem. A*, 1998, **102**, 3315.
- C. Cavallotti, S. Fascella, R. Rota and S. Carra, *Combust. Sci. Technol.*, 2004, **176**, 705.
- C. S. McEnally, L. D. Pfeifferle, A. G. Robinson and T. S. Zwier, *Combust. Flame*, 2000, **123**, 344.
- N. Balucani, G. Capozza, F. Leonori, E. Segoloni and P. Casavecchia, *Int. Rev. Phys. Chem.*, 2006, **25**, 109.
- E. Buonomo and D. C. Clary, *J. Phys. Chem. A*, 2001, **105**, 2694.

- 55 D. C. Clary, E. Buonomo, I. R. Sims, I. W. M. Smith, W. D. Geppert, C. Naulin, M. Costes, L. Cartechini and P. Casavecchia, *J. Phys. Chem. A*, 2002, **106**, 5541.
- 56 M. Frenklach and E. D. Feigelson, *Astrophys. J.*, 1989, **341**, 372.
- 57 X. Gu, Y. Guo, F. Zhang and R. I. Kaiser, *J. Phys. Chem. A*, 2007, **111**, 2980.
- 58 E. Ionescu and S. A. Reid, *THEOCHEM*, 2005, **725**, 45.
- 59 W. M. Jackson, D. S. Anex, R. E. Continetti, B. A. Balko and Y. T. Lee, *J. Chem. Phys.*, 1991, **95**, 7327.
- 60 R. I. Kaiser, C. Ochsensfeld, M. Head-Gordon, Y. T. Lee and A. G. Suits, *Science*, 1996, **274**, 1508.
- 61 A. M. Mebel, *Rev. Mod. Quantum Chem.*, 2002, **1**, 340.
- 62 A. M. Mebel, W. M. Jackson, A. H. H. Chang and S. H. Lin, *J. Am. Chem. Soc.*, 1998, **120**, 5751.
- 63 J. A. Miller and S. J. Klippenstein, *J. Phys. Chem. A*, 2001, **105**, 7254.
- 64 C. Ochsensfeld, R. I. Kaiser, Y. T. Lee, A. G. Suits and M. Head-Gordon, *J. Chem. Phys.*, 1997, **106**, 4141.
- 65 W. K. Park, J. Park, S. C. Park, B. J. Braams, C. Chen and J. M. Bowman, *J. Chem. Phys.*, 2006, **125**, 081101.
- 66 J. A. Miller and S. J. Klippenstein, *J. Phys. Chem. A*, 2003, **107**, 2680.
- 67 J. Aguilera-Iparraguirre, A. D. Boese, W. Klopper and B. Ruscic, *Chem. Phys.*, 2008, **346**, 56.
- 68 A. Bergeat, T. Calvo, F. Caralp, J.-H. Fillion, G. Dorthe and J.-C. Loison, *Faraday Discuss.*, 2001, **119**, 67.
- 69 I. Fernandez and G. Frenking, *Faraday Discuss.*, 2007, **135**, 403.
- 70 M. Hausmann and K. H. Homann, *Ber. Bunsen-Ges.*, 1997, **101**, 651.
- 71 G. Maier, H. P. Reisenauer, W. Schwab, P. Carsky, B. A. Hess, Jr. and L. J. Schaad, *J. Am. Chem. Soc.*, 1987, **109**, 5183.
- 72 J. A. Miller, J. V. Volponi and J.-F. Pauwels, *Combust. Flame*, 1996, **105**, 451.
- 73 A. Mohajeri and M. J. Jenabi, *THEOCHEM*, 2007, **820**, 65.
- 74 H. P. Reisenauer, G. Maier, A. Riemann and R. W. Hoffman, *Angew. Chem.*, 1984, **96**, 596.
- 75 R. A. Seburg, J. T. DePinto, E. V. Patterson and R. J. McMahon, *J. Am. Chem. Soc.*, 1995, **117**, 835.
- 76 R. A. Seburg, E. V. Patterson and R. J. McMahon, *J. Am. Chem. Soc.*, 2009, **131**, 9442.
- 77 R. A. Seburg, E. V. Patterson, J. F. Stanton and R. J. McMahon, *J. Am. Chem. Soc.*, 1997, **119**, 5847.
- 78 L. B. Harding, S. J. Klippenstein and Y. Georgievskii, *J. Phys. Chem. A*, 2007, **111**, 3789.
- 79 C. A. Taatjes, S. J. Klippenstein, N. Hansen, J. A. Miller, T. A. Cool, J. Wang, M. E. Law and P. R. Westmoreland, *Phys. Chem. Chem. Phys.*, 2005, **7**, 806.
- 80 A. Bhargava and P. R. Westmoreland, *Combust. Flame*, 1998, **113**, 333.
- 81 J. D. Bittner, *PhD Thesis*, MIT, 1981.
- 82 G. E. Oulundsen, *PhD Thesis*, Univ. Massachusetts, 1999.
- 83 P. R. Westmoreland, J. B. Howard, J. P. Longwell and A. M. Dean, *AICHE J.*, 1986, **32**, 1971.
- 84 A. Canosa, I. R. Sims, D. Travers, I. W. M. Smith and B. R. Rowe, *Astron. Astrophys.*, 1997, **323**, 644.
- 85 J.-C. Loison and A. Bergeat, *Phys. Chem. Chem. Phys.*, 2009, **11**, 655.
- 86 L. Vereecken, K. Pierloot and J. Peeters, *J. Chem. Phys.*, 1998, **108**, 1068.
- 87 R. Guadagnini, G. C. Schatz and S. P. Walch, *J. Phys. Chem. A*, 1998, **102**, 5857.
- 88 L. Vereecken and J. Peeters, *J. Phys. Chem. A*, 1999, **103**, 5523.
- 89 T. L. Nguyen, A. M. Mebel, S. H. Lin and R. I. Kaiser, *J. Phys. Chem. A*, 2001, **105**, 11549.
- 90 F. Goulay, A. J. Trevitt, G. Meloni, T. M. Selby, D. L. Osborn, C. A. Taatjes, L. Vereecken and S. R. Leone, *J. Am. Chem. Soc.*, 2009, **131**, 993.
- 91 H.-J. Deyerl, I. Fischer and P. Chen, *J. Chem. Phys.*, 1999, **111**, 3441.
- 92 L. R. McCunn, B. L. FitzPatrick, M. J. Krisch, L. J. Butler, C.-W. Liang and J. J. Lin, *J. Chem. Phys.*, 2006, **125**, 133306.
- 93 S. J. Goncher, D. T. Moore, N. E. Sveum and D. M. Neumark, *J. Chem. Phys.*, 2008, **128**, 114303.
- 94 A compilation of rate constants is given in <http://kinetics.nist.gov/kinetics/index.jsp>.
- 95 H. Thiesemann, J. MacNamara and C. A. Taatjes, *J. Phys. Chem. A*, 1997, **101**, 1881.
- 96 W. Boullart, K. Devriendt, R. Borms and J. Peeters, *J. Phys. Chem.*, 1996, **100**, 998.
- 97 K. McKee, M. A. Blitz, K. J. Hughes, M. J. Pilling, H.-B. Qian, A. Taylor and P. W. Seakins, *J. Phys. Chem. A*, 2003, **107**, 5710.
- 98 *Atomic and Molecular Beam Methods*, ed. G. Scoles, Oxford University Press, Oxford, 1988.
- 99 P. Casavecchia, G. Capozza and E. Segoloni, *Adv. Ser. Phys. Chem.*, 2004, **14**, 329.
- 100 R. I. Kaiser, *Chem. Rev.*, 2002, **102**, 1309.
- 101 K. Liu, *J. Chem. Phys.*, 2006, **125**, 132307.
- 102 J. A. Miller and C. T. Bowman, *Prog. Energy Combust. Sci.*, 1989, **15**, 287.
- 103 J. A. Miller, R. J. Kee and C. K. Westbrook, *Annu. Rev. Phys. Chem.*, 1990, **41**, 345.
- 104 C. H. Wu and R. D. Kern, *J. Phys. Chem.*, 1987, **91**, 6291.
- 105 R. D. Kern, C. H. Wu, J. N. Yong, K. M. Pamidimukkala and H. J. Singh, *Energy Fuels*, 1988, **2**, 454.
- 106 J. Peeters, W. Boullart and K. Devriendt, *J. Phys. Chem.*, 1995, **99**, 3583.
- 107 J. Peeters, *Bull. Soc. Chim. Belg.*, 1997, **106**, 337.
- 108 R. A. Abramovich, *Editor Reactive Intermediates*, 1980, vol. 1.
- 109 H. E. Matthews and W. M. Irvine, *Astrophys. J.*, 1985, **298**, L61.
- 110 P. Thaddeus, J. M. Vrtilik and C. A. Gottlieb, *Astrophys. J.*, 1985, **299**, L63.
- 111 J. Cernicharo, C. A. Gottlieb, M. Guelin, T. C. Killian, G. Paubert, P. Thaddeus and J. M. Vrtilik, *Astrophys. J.*, 1991, **368**, L39.
- 112 R. I. Kaiser, C. Ochsensfeld, D. Stranges, M. Head-Gordon and b. p. Y. T. Lee, *Faraday Discuss.*, 1998, **109**, 183.
- 113 E. Herbst, H.-H. Lee, D. A. Howe and T. J. Millar, *Mon. Not. R. Astron. Soc.*, 1994, **268**, 335.
- 114 T. B. H. Kuiper, J. B. Whiteoak, R. S. Peng, W. L. Peters, III and J. E. Reynolds, *Astrophys. J.*, 1993, **416**, L33.
- 115 R. V. Yelle, F. Herbert, B. R. Sandel, R. J. Vervack, Jr. and T. M. Wentzel, *Icarus*, 1993, **104**, 38.
- 116 V. A. Krasnopolsky and D. P. Cruikshank, *J. Geophys. Res., [Planets]*, 1995, **100**, 21.
- 117 P. P. Lavvas, A. Coustenis and I. M. Vardavas, *Planet. Space Sci.*, 2008, **56**, 67.
- 118 X. B. Gu, Y. Guo, H. Chan, E. Kawamura and R. I. Kaiser, *Rev. Sci. Instrum.*, 2005, **76**, 116103.
- 119 X. B. Gu, Y. Guo, E. Kawamura and R. I. Kaiser, *Rev. Sci. Instrum.*, 2005, **76**, 083115.
- 120 Y. Guo, X. Gu, E. Kawamura and R. I. Kaiser, *Rev. Sci. Instrum.*, 2006, **77**, 034701.
- 121 Y. Guo, X. Gu and R. I. Kaiser, *Int. J. Mass Spectrom.*, 2006, **249/250**, 420.
- 122 W. S. McGivern, O. Sorkhabi, A. G. Suits, A. Derecskei-Kovacs and S. W. North, *J. Phys. Chem. A*, 2000, **104**, 10085.
- 123 P. Zou, J. Shu, T. J. Sears, G. E. Hall and S. W. North, *J. Phys. Chem. A*, 2004, **108**, 1482.
- 124 R. Atkinson, D. L. Baulch, R. A. Cox, R. F. Hampson, Jr., J. A. Kerr and J. Troe, *J. Phys. Chem. Ref. Data*, 1992, **21**, 1548.
- 125 A. M. Mebel, *Florida International University*, unpublished results, 2010.
- 126 M. Vernon, *PhD Thesis*, University of California, 1981.
- 127 M. S. Weiss, *PhD Thesis*, University of California, 1986.
- 128 M. Danielsson, P. Erman, A. Hishikawa, M. Larsson and E. Rachlew-Kaellne, *J. Chem. Phys.*, 1993, **98**, 9405.
- 129 <http://www.sri.com/psd/libbase/>.
- 130 R. D. Levine, *Molecular Reaction Dynamics*, Cambridge University Press, Cambridge, UK, 2005, p. 568.
- 131 R. I. Kaiser, Y. T. Lee and A. G. Suits, *J. Chem. Phys.*, 1996, **105**, 8705.
- 132 J. Vazquez, M. E. Harding, J. Gauss and J. F. Stanton, *J. Phys. Chem. A*, 2009, **113**, 12447.